| | | | | | |
|---|---|---|---|---|---|
| Jo J, Nagaya N, Miyahata Y, Kataoka M, Harada-shiba M, Kangawa K, Tabata Y, | Transplantation of genetically engineered mesenchymal stem cells improves cardiac function in rats with myocardial infarction: benefit of a novel nonviral vector, cationized dextran. | Tissue Engineering | 13(2) | 313-322 | 2007 |
| K. Sugisaki, T. Usui, N. Nishiyama, W-D Jang, Y. Yanagi, S. Yamagami, S. Amano, K. Kataoka | Photodynamic therapy for corneal neovascularization using polymeric micelles encapsulating dendrimer porphyrins. | Invest. Ophth. Vis. Sci | | | in press |
| S. Wu, S. Murai, K. Kataoka, M. Miyagishi | Yin Yang 1 induces Transcriptional Activity of p73 through Cooperation with E2F1. | Biochem. Bioph. Res. Co. | 365 (1) | 75-81 | 2008 |
| A. Harada, K. Kataoka | Selection between block- and homo-polyelectrolytes through polyion complex formation in aqueous medium. | Soft Matter | 4 (1) | 162-167 | 2008 |
| Y. Imai, E. Kaneko, T. Asano, M. Kumagai, M. Ai, A. Kawakami, K. Kataoka, K. Shimokado | A novel contrast medium detects increased permeability of rat injured carotid arteries in magnetic resonance T2 mapping imaging. | J Athero. Throm | 14 (2) | 65-71 | 2007 |
| S. Hiki, K. Kataoka | A Facile Synthesis of Azido-Terminated Heterobifunctional Poly(ethylene glycol)s for "Click" Conjugation. | Bioconjugate. Chem. | 18 (6) | 2191-2196 | 2007 |
| Y. Li, W. -D. Jang, N. Nishiyama, A. Kishimura, S. Kawauchi, Y. Morimoto, S. Miake, T. Yamashita, M. Kikuchi, T. Aida, K. Kataoka | Dendrimer Generation Effects on Photodynamic Efficacy of Dendrimer Porphyrins and Dendrimer-Loaded Supramolecular Nanocarriers. | Chem. Mater. | 19 (23) | 5557-5562 | 2007 |

| | | | | | |
|---|---|---|---|---|---|
| K. Masago, K. Itaka, N. Nishiyama, U. Chung, K. Kataoka | Gene delivery with biocompatible cationic polymer:Pharmacogenomic analysis on cell bioactivity | Biomaterials | 28 (34) | 5169-5175 | 2007 |
| A. Kawamura, A. Harada, K. Kono, K. Kataoka | Self-Assembled Nano - Bioreactor from Block Ionomers with Elevated and Stabilized Enzymatic Function | Bioconjugate Chem. | 18 (5) | 1555-1559 | 2007 |
| M. Nakanishi, J. -S. Park, W. -D. Jang, M. Oba, K. Kataoka | Study of the quantitative aminolysis reaction of poly(beta-benzyl L-aspartate) (PBLA) as a platform polymer for functionality materials. | React. Funct. Polym. | 67 (11) | 1361-1372 | 2007 |
| M. P. Xiong, Y. Bae, S. Fukushima, M. L. Forrest, N. Nishiyama, K. Kataoka, G. S. Kwon, | pH-Responsive Multi-PEGylated Dual Cationic Nanoparticles Enable Charge Modulations for Safe Gene Delivery | ChemMedChem. | 2 (9) | 1321-1327 | 2007 |
| M. Oishi, Y. Nagasaki, N. Nishiyama, K. Itaka, M. Takagi, A. Shimamoto, Y. Furuichi, K. Kataoka | Enhanced Growth Inhibition of Hepatic Multicellular Tumor Spheroids by Lactosylated Poly(ethylene glycol)-siRNA Conjugate Formulated in PEGylated Polyplexes | ChemMedChem | 2 (9) | 1290-1297 | 2007 |
| 西山伸宏、片岡一則 | 人工ウィルスの実現に向けた高分子ミセル型ベクターの設計 | 細胞工学 | Vol. 27, No. 1 | 56-61 | 2008 |
| K. Miyata, S. Fukushima, N. Nishiyama, Y. Yamasaki, K. Kataoka | PEG-based block catiomers possessing DNA anchoring and endosomal escaping functions to form polyplex micelles with improved stability and high transfection efficacy | J. Control. Release | 122 (3) | 252-260 | 2007 |

| | | | | | |
|---|---|---|---|---|---|
| M. Oba, S. Fukushima, N. Kanayama, K. Aoyagi, N. Nishiyama, H. Koyama, K. Kataoka | Cyclic RGD peptide-conjugated polyplex micelles as a targetable gene delivery system directed to cells possessing alphavbeta3 and alphavbeta5 integrins. | Bioconjugate Chem. | 18 (5) | 1415-1423 | 2007 |
| H. Cabral, N. Nishiyama, K. Kataoka | Optimization of (1,2-diamino-cyclohexane)platinum(II) -loaded polymeric micelles directed to improved tumor targeting and enhanced antitumor activity | J. Control. Release | 121 (3) | 146-155 | 2007 |
| M. Han, Y. Bae, N. Nishiyama, K. Miyata, M. Oba, K. Kataoka | Transfection Study Using Multicellular Tumor Spheroids for Screening Non-viral Polymeric Gene Vectors with Low Cytotoxicity and High Transfection Efficiencies. | J. Control. Release | 121 (1-2) | 38-48 | 2007 |
| S. Takae, Y. Akiyama, Y. Yamasaki, Y. Nagasaki, K. Kataoka | Colloidal Au Replacement Assay for Highly Sensitive Quantification of Low Molecular Weight Analytes by Surface Plasmon Resonance | Bioconjugate Chem. | 18(4) | 1241-1245 | 2007 |
| Y. Bae, N. Nishiyama, K. Kataoka | n Vivo Antitumor Activity of the Folate - Conjugated pH-Sensitive Polymeric Micelle Selectively Releasing Adriamycin in the Intracellular Acidic Compartments | Bioconjugate Chem. | 18(4) | 1131-1139 | 2007 |
| A. Kishimura, A. Koide, K. Osada, Y. Yamasaki, K. Kataoka | Encapsulation of myoglobin in PEGylated polyion complex vesicles made from a pair of oppositely charged block ionomers: a physiologically available oxygen carrier | Angew. Chem. Int. Ed. | 46(32) | 6085-6088 | 2007 |
| K. Itaka, S. Ohba, K. Miyata, H. Kawaguchi, K. Nakamura, T. Takato, U. -I. Chung, K. Kataoka | Bone regeneration by regulated in vivo gene transfer using biocompatible polyplex nanomicelles | Mol Ther. | 15 (9) | 1655-1662 | 2007 |

| | | | | | |
|---|---|---|---|---|---|
| T. Satomi, Y. Nagasaki, H. Kobayashi, H. Otsuka, K. Kataoka | Density Control of Poly(ethylene glycol)Layer To Regulate Cellular Attachment | Langmuir | 23(12) | 6698-6703 | 2007 |
| M. Oishi, H. Hayashi, K. Itaka, K. Kataoka, Y. Nagasaki | pH-Responsive PEGylated nanogels as targetable and low invasive endosomolytic agents to induce the enhanced transfection efficiency of nonviral gene vectors | Colloid. Polym. Sci. | 285 | 1055-1060 | 2007 |
| D. Akagi, M. Oba, H. Koyama, N. Nishiyama, S. Fukushima, T. Miyata, H. Nagawa, K. Kataoka | Biocompatible micellar nanovectors achieve efficient gene transfer to vascular lesions without cytotoxicity and thrombus formation | Gene Ther. | 14 (13) | 1029-1038 | 2007 |
| J. K. Oh, D. J. Siegwart, H. -I Lee, G. Sherwood, L. Peteanu, J. O. Hollinger, K. Kataoka, K. Matyjaszewski | Biodegradable Nanogels Prepared by Atom Transfer Radical Polymerization as Potential Drug Delivery Carriers: Synthesis, Biodegradation, in Vitro Release, and Bioconjugation. | J. Am. Chem. Soc. | 129 (18) | 5939-5945 | 2007 |
| J. -S. Park, K. Kataoka | Comprehensive and accurate control of thermosensitivity of poly(2-alkyl-2-oxazoline)s via well-defined gradient or random copolymerization | Macromolecules | 40 (10) | 3599-3609 | 2007 |
| Y. Lee, S. Fukushima, Y. Bae, S. Hiki, T. Ishii, K. Kataoka | A Protein Nanocarrier from Charge-Conversion Polymer in Response to Endosomal pH | J. Am. Chem. Soc. | 129 (17) | 5362-5363 | 2007 |
| I. A. Khalil, K. Kogure, S. Futaki, S. Hama, H. Akita, M. Ueno, H. Kishida, M. Kudoh, Y. Mishina, K. Kataoka, M. Yamada, H. Harashima | Octaarginine-modified multifunctional envelope-type nanoparticles for gene delivery | Gene Ther. | 14 (8) | 682-689 | 2007 |
| M. R. Kano, Y. Bae, C. Iwata, Y. Morishita, M. Yashiro, M. Oka, T. Fujii, A. Komuro, K. Kiyono, M. Kamiishi, K. Hirakawa, Y. Ouchi, N. Nishiyama, K. Kataoka, K. Miyazono | Improvement of cancer-targeting therapy, using nanocarriers for intractable solid tumors by inhibition of TGF-beta signaling | P. Natl. Acad. Sci. USA. | 104 (9) | 3460-3465 | 2007 |

| | | | | | |
|---|---|---|---|---|---|
| M. Kumagai, Y. Imai, T. Nakamura, Y. Yamasaki, M. Sekino, S. Ueno, K. Hanaoka, K. Kikuchi, T. Nagano, E. Kaneko, K. Shimokado, K. Kataoka | Iron hydroxide nanoparticles coated with poly(ethylene glycol)-poly(aspartic acid) block copolymer as novel magnetic resonance contrast agents for in vivo cancer imaging. | Colloids Surf., B Biointerfaces | 56 | 174-181 | 2007 |
| J.-S. Park, Y. Akiyama, Y. Yamasaki, K. Kataoka | Preparation and characterization of polyion complex micelles with a novel thermosensitive poly(2-isopropyl-2-oxazoline) shell via the complexation of oppositely charged block | Langmuir | 23 (1) | 138-146 | 2007 |
| W. -D. Jang, N. Nishiyama, K. Kataoka | Preparation of naphthalocyanine dendrimer loaded polyion complex micelle for photodynamic therapy | Key Eng. Mater. | 342-343(Advanced Biomaterials VII) | 465-468 | 2007 |
| Ichi I, Takashima Y, Adachi N, Nakahara K, Kamikawa C, Harada-Shiba M , Kojo S, | Effects of Dietary Cholesterol on Tissue Ceramides and Oxidation Products of Apolipoprotein B-100 in ApoE-Deficient Mice | Lipids | 42 | 893-900 | 2007 |

J Mater Sci (2008) 43:2442–2446
DOI 10.1007/s10853-007-2040-9



# Hydrothermal treatment of glycine and adiabatic expansion cooling: implications for prebiotic synthesis of biopolymers

**Yasuhiro Futamura · Kouki Fujioka · Kenji Yamamoto**

Received: 15 November 2006 / Accepted: 20 July 2007 / Published online: 13 November 2007


**Abstract** There have been several studies on biopolymer synthesis under hydrothermal conditions. The conventional hydrothermal methods make it possible to synthesize only a dipeptide and short oligopeptides as well as cyclo-dimer, from amino acids. As these studies that were applied with various quenching methods suggested the importance of quenching rate from hydrothermal conditions, rapid quenching could avoid hydrolysis of the oligomers that had already been synthesized under hydrothermal conditions. In this study, therefore, we designed a novel hydrothermal flow reactor adopted with adiabatic expansion cooling system from the reason that it was thought to be one of the most rapid quenching methods. It mimics geysers, fumaroles, hot springs, and volcanic eruptions. Once aqueous solutions of monomers were treated at high temperature and pressure, the solutions were released into the atmosphere through an orifice to be depressurized and cooled down simultaneously with the Joule–Thomson effect. We demonstrated oligomerization of glycine up to decamer ($Gly_{10}$) by using the flow reactor, which had never been yielded with any other quenching methods. This suggests that rapid quenching methods under non-equilibrium conditions such as adiabatic expansion cooling is an efficient way to produce long oligomers connected by covalent bonds via dehydration condensation.

Y. Futamura · K. Fujioka · K. Yamamoto (✉)
International Clinical Research Center, Research Institute, International Medical Center of Japan, 1-21-1 Toyama, Shinjuku-ku, Tokyo 162-8655, Japan
e-mail: backen@ri.imcj.go.jp

Y. Futamura
Department of Bioactive Molecules, National Institute of Infectious Diseases, 1-23-1 Toyama, Shinjuku-ku, Tokyo 162-8640, Japan

K. Yamamoto
Institute of Multidisciplinary Research for Advanced Materials, Tohoku University, 2-1-1 Katahira, Aoba-ku, Sendai 980-8577, Japan

## Introduction

### Origins of life and prebiotic synthesis of its component

On the basis of phylogenetic analyses, hyperthermophiles are located near the root of the phylogenetic tree. From the view of origins of life, the last common ancestor is thought to be a hyperthermophile [1]. In the context, the first living cell might have been born under hydrothermal conditions on the earth. However, where and how were the components of living cells synthesized?

Living cells are composed with water, inorganics, and organics such as proteins, nucleic acids, polysaccharides, and so on. Such organics are composed with monomer of amino acids, nucleotides, sugars, respectively (Fig. 1). The onset of polymerization must have been a major step in the chemical evolution that formed the precursors of life. In this paper, we'd like to focus on polymer synthesis from monomers under hydrothermal conditions.

### Prebiotic synthesis of biopolymers in deep sea or in geysers?

Submarine "Alvin" discovered chemoautotrophic communities in a hydrothermal vent in deep sea of Galapagos Rift in 1977 [2, 3]. The temperature would be 100–400 °C and the pressure should depend on the hydraulic pressure

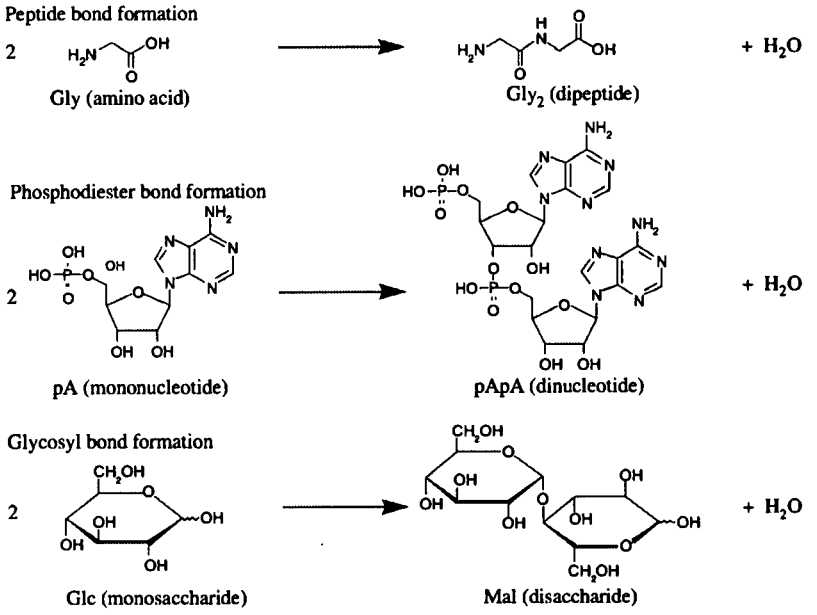


**Fig. 1** Dehydration condensation of various monomers: amino acids, nucleotides, and saccharides

that is 25 MPa at a depth of 2,500 m. After then, hydrothermal vents are thought to be one of the candidates of place of origins of life and the components of living cells would be also synthesized from monomers there [4].

Imai and his colleagues tried to polymerize an amino acid using a flow reactor that simulates a submarine hydrothermal vent. As the results, up to trimer of oligoglycine were yielded without any catalyst added [4–7].

Now, we report a novel flow reactor dealing with subcritical and supercritical water for synthesizing oligopeptides from amino acids. The adiabatic expansion method for quenching and depressurizing the system was adopted to reduce the hydrolysis reaction of products. In almost all the previous studies the temperature and pressure of the system or the reaction time are often focused on. On the other hand, there is hardly any knowledge of methods of quenching and depressurizing the system. We considered these processes important.

In this study we worked on the reaction where glycine, the simplest amino acid, is formed into oligoglycines. After heating and pressurizing the glycine aqueous solution without any catalysts, it was quenched and depressurized with the adiabatic expansion method. The diglycine was produced about 45 times as much as in a previous study using water-cooled method for quenching the solution. It suggests that when the oligomer produced in water at high temperature and under high pressure was quenched, it was not hydrolyzed because of the higher rate of quenching. What is more, the concentration of linear-dimer was more than that of cyclo-dimer. It suggests our method was more suitable to make long peptides from amino acids. Actually we obtained longer chains of peptides up to decamer, which were not obtained in the previous studies.

The flow reactor in the previous studies simulated submarine hydrothermal vents in deep sea. On the other hand, the flow reactor with adiabatic expansion cooling simulates geysers and hot springs. Such a rapid quenching environment would be suitable for synthesis of hydrolytic compounds such as biopolymers.

## Experimental details

The flow diagram of an experimental apparatus we designed is shown in Fig. 2. The apparatus had two reservoirs, one was for water and the other was for sample solution. Water was pressurized by the pump P-1 and was heated with the pre-heating unit. On the other hand, the pump P-2 pressurized sample solution. In order to raise the temperature of sample solution rapidly, sample solution and heated water were mixed together in the interflow block whose temperature was monitored with the thermoelectric couple TI-1. The needle valve made it feasible that the solution was quenched and depressurized more rapidly than by a water-cooling unit, a conventional method. Therefore it was expected that the hydrolysis or the decomposition of products would be suppressed during quenching and depressurizing the solution.

HPLC and LC-Mass analyses of oligoglycines were performed as described in Fig. 3.

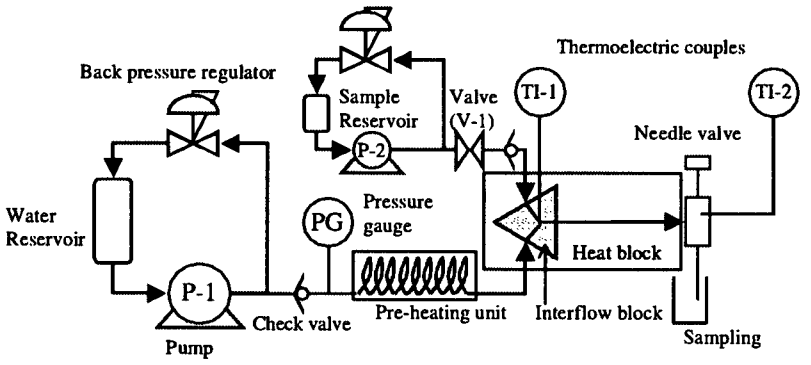


**Fig. 2** The experimental apparatus adopted for an adiabatic expansion cooling with a needle valve to reduce the hydrolysis reaction of products; This flow reactor was designed to endure up to 40 MPa and 500 °C. Almost all the parts that contacted with the solution were made of stainless steel SUS316. A stainless tube, which a heat block kept heated, was placed between an interflow block and an inlet of a needle valve. The volume of the tube was 1.5 mL. The gap of needle valve is about 10 $mm^2$

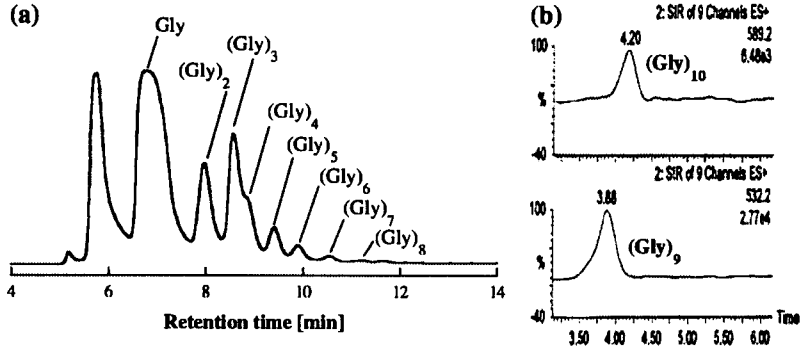


**Fig. 3** (**a**) A high performance liquid chromatography (HPLC) profiles of the products in the sample that yielded from 0.1 mol/L glycine aqueous solution at 270 °C and 10 MPa and (**b**) Selected Ion Monitoring (SIM) mass chromatograms of decaglycine (top) and nonaglycine (bottom); $(Gly)_i$ denotes i-mer of glycine. The chromatograms were obtained from a Waters HPLC and LC/Mass spectrometry system respectively, with the use of a same reverse-phase column (Waters Xterra MS $C_{18}$ 2.5 mm; 4.6 × 50 mm). Aqueous solution containing 50 mM $KH_2PO_4$ and 7.2 mM $C_6H_{13}SO_3Na$ (pH = 2.5) was used as a mobile phase in the condition for (**a**). The UV detector monitored the absorbance at 200 nm. In the condition for (**b**), aqueous solution of 1 mM $C_5F_{11}COOH$ was used as a mobile phase and the mass chromatograms of the oligoglycines were detected in Selected Ion Recording (SIR) mode

## Results and discussion

### Oligomerization of glycine

So far, there have been several studies on oligomerization of amino acids in subcritical water. Nevertheless, in most of the studies [4–7], oligomerization reaction did not occur efficiently.

Using the flow reactor with adiabatic expansion cooling (Fig. 2), after pressured, glycine aqueous solution was mixed into pre-heated water to make it reach the desired condition of concentration and temperature in the reactor, and it was quenched with adiabatic expansion. As shown in Fig. 3, we obtained various oligoglycines up to decaglycine ($Gly_{10}$) that had never been obtained with any other cooling methods [4–8].

### Polymerization or circulation

It was found that the reaction solution contained diglycine and cyclo-diglycine (diketopiperazine) as its products. These concentrations were 0.078 and 0.015 mM respectively, which was calculated by HPLC chromatogram areas in Fig. 3. The concentration of the diglycine was 45 times as much as that in the previous study by Islam et al. [7]. Moreover, in comparing our study with the previous studies, we found an interesting fact about the ratios of linear-dimer against cyclo-dimer.

After the experiment of Imai et al. [4], not a few works on the polymerization of the amino acids has been done with the supercritical and subcritical water and supported the formation of cyclo-dimer. In all of these experiments, cyclo-dimer was detected more than the linear dimer [4–7].

**Table 1** Ratio of diglycine to cyclo-diglycine after hydrothermal treatment of glycine

| Reference | Reaction condition | | | Products conclusion |
|---|---|---|---|---|
| | P (MPa) | T (K) | Glycine (Raw material) (mM) | [cyclo-diglycine]/[linear-diglycine] |
| Imai et al. [4] | 24 | 498 | 100 | 0.2 |
| Ogata et al. [6] | 24 | 523 | 100 | 0.17 |
| Alargov et al. [5] | 22 | 623 | 65 | 0.23 |
| Islam et al. [7] | 25 | 523 | 100 | 0.096 |
| This study | 24 | 523 | 100 | 5.2 |

Table 1 shows the results obtained from the different papers with their own devices under the different conditions. In all the previous studies, the ratios were less than one, but our result was opposite, the concentration of linear-dimer was more than that of cyclo-dimer. It meant that our experiment, especially adopting the process of depressurizing and quenching, was more suitable to make long peptides from amino acids because the seed of polymer was thought to be linear-multimer like diglycine. As a result, our apparatus using the needle valve had a possibility to be proper for making the hydrolytic compounds such as biopolymers.

The equilibrium reaction among glycine, diglycine, and cyclo-diglycine is shown in Fig. 4. Cyclo-dimer is formed via intramolecular condensation reaction of linear dimer, called unimolecular reaction, whereas linear oligomers are formed via intermolecular condensation of monomers and/or oligomers. Bimolecular reaction depends on the concentration of reactants. Adiabatic expansion cooling may contribute to increasing the concentration of reactants of bimolecular reaction.

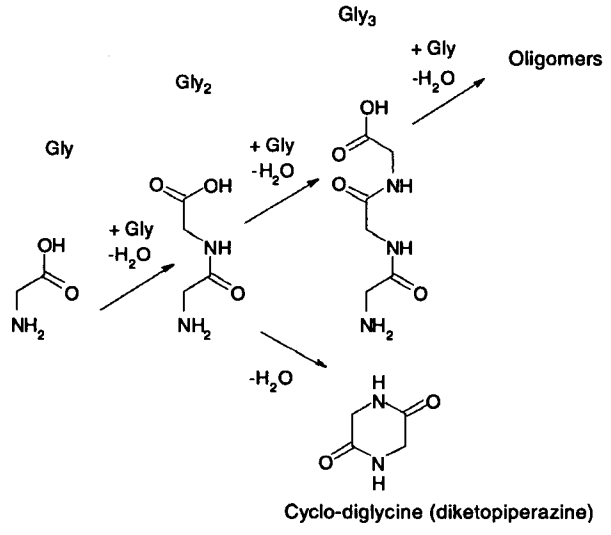


**Fig. 4** Oligomerization of glycines and intramolecular condensation of diglycine

These results led us to the speculation that the amino acids could be polymerized linearly in the high pressure and high temperature water, but as for the cyclo-multimer, the polymerization would stop at the cyclo-dimer (Fig. 4). The generation of the cyclo-dimer from the monomer amino acids will compete the generation of the linear multimer. If the polymerization of the amino acids might be necessary for the initiation of the origin of life, this result leads us to a paradoxical problem.

## Perspectives

Considering prebiotic chemical evolution, biopolymer syntheses have a common point: dehydration condensation of monomers. Dehydration condensation is a common reaction to form hydrolytic bonds between monomers, such as amide bond formation of oligopeptides, phosphoester bond formation of oligonucleotides, glycosyl bond formation of oligosaccharides, and acyl bond formation of lipids. Non-equilibrium cooling from hydrothermal conditions would be efficient for various types of dehydration condensation reaction.

**Acknowledgements** We thank Mr. Tomomasa Goto and Prof. Yukio Yamaguchi, Department of Chemical System Engineering, School of Engineering, The University of Tokyo for hydrothermal experiments and useful discussion, and Mr. Satoru Aizawa and Mr. Shinya Harada, AKICO Co. for the design and construction of the experimental apparatus. This work was partly supported by the research grants for *Learning from Nature for Production 2002–2003* from Sekisui Chemical Co., LTD., and by Grants-in-Aid for Scientific Research from the Ministry of Education, Culture, Sports, Science and Technology.

## References

1. Woese CR, Kandler O, Wheelis ML (1990) Proc Natl Acad Sci USA 87:4576
2. Corliss JB, Ballard RD (1977) Natl Geogr 152:441
3. Corliss JB, Dymond J, Gordon LI, Edmond JM, Von Herzen RP, Ballard RD, Green K, Williams D, Bainbridge A, Crane K, Van Andel TH (1979) Science 203:1073
4. Imai E, Honda H, Hatori K, Brack A, Matsuno K (1999) Science 283:831

5. Alargov DK, Deguchi S, Tsujii K, Horikoshi K (2002) Orig Life Evol Biosph 32:1
6. Ogata Y, Imai E, Honda H, Hatori K, Matsuno K (2000) Orig Life Evol Biosph 30:527
7. Islam MN, Kaneko T, Kobayashi K (2003) Bull Chem Soc Jpn 76:1171
8. Goto T, Futamura Y, Yamaguchi Y, Yamamoto K (2005) J Chem Eng Jpn 38:295

# NOTES

## Separation of Murine Neutrophils and Macrophages by Thermoresponsive Magnetic Nanoparticles

**Akiyoshi Hoshino,[†,‡] Noriyuki Ohnishi,[§] Masato Yasuhara,[‡] Kenji Yamamoto,[†,‡] and Akihiko Kondo*[,∥]**

International Clinical Research Center, Research Institute, International Medical Center of Japan, Tokyo, Japan, Department of Pharmacokinetics and Pharmacodynamics, Hospital Pharmacy, Tokyo Medical and Dental University Graduate School, Tokyo, Japan, Magnabeat Inc., Goi Research Center, Chisso Petrochemical Corporation, Chiba, Japan, and Department of Chemical Science and Engineering, Faculty of Engineering, Kobe University, Kobe, Japan

Magnetic particles have been used widely in both biotechnological and medical fields, including for immunoassay, enzyme immobilization, drug transport, and immunological diagnosis. Especially particles with bioactive molecules such as antibodies and streptavidin are very useful tools for cell separation. Here we report affinity selection of neutrophils and macrophages from peritoneal inflammatory cells performed by thermoresponsive magnetic nanoparticles conjugated with macrophage-specific anti-F4/80 antibody. The magnetic nanoparticles, which are capped with thermoresponsive polymers, are aggregated by heating the particles over 30 °C and show their intrinsic magnetism. The neutrophils are concentrated approximately 90% by these magnetic nanoparticles without any activation, indicating that this novel cell separation method could fulfill a wide range of applications in analysis of the isolation of fragile cells such as neutrophils.

With the development of nanotechnology, nanometer-sized products that are smaller than several hundred nanometers have been applied in almost all areas of science and technology. The nanometer-sized products, including carbon nanotubes, fullerene derivatives, and nanocrystal quantum dots, are widely used as novel tools in various fields including the materials engineering, electronics, plastics, automobile, aviation, and aerospace industries (*1*). In recent years, nanobiotechnology, which is a fused research field of biotechnology and nanotechnology, has been widely expected to apply the fruits of advanced nanomaterials to even the fields of cellular and molecular biology (*2*−*4*) and basic and clinical medicine (*5*−*13*). In particular, nanoparticles exert their intrinsic properties based on nanometer-sized effect that is generated from increased surface area per their volume. Therefore, research reagents with nanoparticles are expected to show higher specificity for the reaction and shorter reaction time compared with conventional ones. In the case of magnetic particles, a smaller particle is the more effective to exert its magnetic reactivity, because the sensitivity of the magnetic particle is defined by the particle surface area. However, a small magnetic particle less than 1 μm hardly responds to a magnetic field because it has less magnetism due to its extra small size. We capped these magnetic nanoparticles with thermoresponsive polymers in order to exert much stronger magnetism by heat-mediated aggregation (*14*). By this surface modification we succeeded in gathering magnetic nanoparticles whenever we want.

Neutrophils are known to be the primary responding immune cells in the case of acute protection against microorganisms (*15*). The lifetimes of neutrophils are known to be a couple of days, whereas monocytes/macrophages live more than several months. Neutrophils act as phagocytic cells when they encounter microorganisms (*16*). In some case, neutrophils release cellular enzymes such as hydrases, myeloperoxidases, elastases, and other lysosomal enzymes from their granules in order to kill bacteria, fungi, and other microbes (*17*−*20*). Therefore, neutrophils are too sensitive to collect without inducing any activation (*21*).

In this method, we demonstrate a novel method to separate neutrophils from acute inflammatory neutrophils and macrophages by thermoreactive magnetic nanoparticles.

### Materials and Methods

**Preparation of Thermoresponsive Magnetic Nanoparticle with Antibody.** A solution of thermoresponsive magnetic nanoparticles conjugated with Therma-Max LSA Streptavidin (30) was a gift from Magnabeat Incorporated (Chiba, Japan). The effective particle size distribution in aqueous solutions was measured by the DLS method with the particle characterizer Zeta Sizer-Nano ZS (Malvern Instruments, Malvern, Worcestershire, U.K.). The temperature response of the thermoresponsive magnetic nanoparticles was measured using a spectrophotometer equipped with a water bath to control the temperature of the cuvette.

* To whom correspondence should be addressed. Tel: +81-78-803-6196. E-mail: akondo@kobe-u.ac.jp.
† International Medical Center of Japan.
‡ Tokyo Medical and Dental University Graduate School.
§ Magnabeat Inc.
∥ Kobe University.

10.1021/bp070185e CCC: $37.00 
Published on Web 10/20/2007

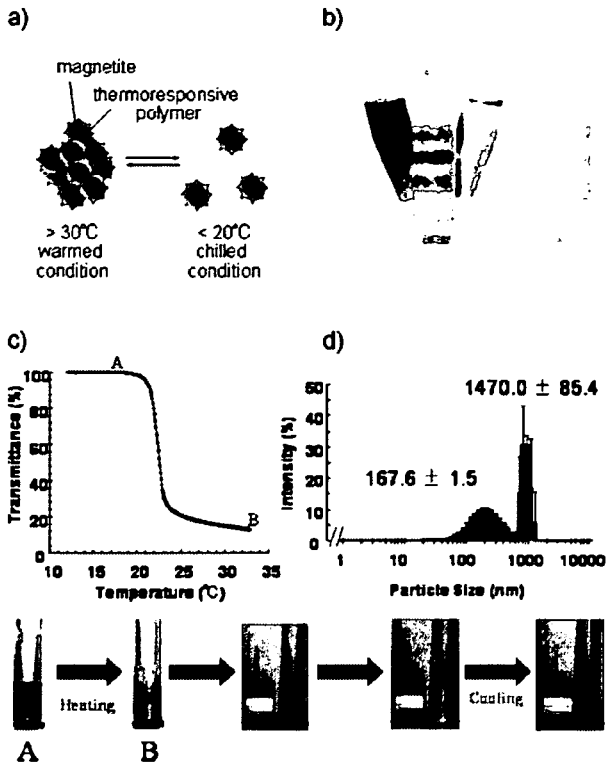


**Figure 1.** Properties of thermoresponsive magnetic nanoparticles. (a) Schematic model for the structure of thermoresponsive magnetic nanoparticles. (b) Comparison of accumulation of the magnetic nanoparticles under the magnetic field. The photos were captured after 30 s in the magnetic field: (left) <20 °C chilled condition, (right) >30 °C warmed condition. (c) Thermal transmittance of the magnetic nanoparticles. The transparent nanoparticle solution (A) becomes turbid (B) by heating. (d) Size distribution of magnetic nanoparticle measured by DLS methods. The particles at chilled condition show diameters of 167.6 ± 1.5 nm at 10 °C (blue column), whereas at 40 °C they are 1470.0 ± 85.4 nm (red column).

The thermoresponsive magnetic nanoparticles used for neutrophil separation were prepared as follows. A 10 $\mu$g portion of Therma-Max LSA Streptavidin (30) magnetic nanoparticles (4 mg/mL solution) conjugated with streptavidin was mixed with 20 $\mu$g of biotinylated anti-F4/80 monoclonal Ab (100 $\mu$g/mL, Caltag Laboratories, Burlingame, CA) and incubated on ice for 30 min for conjugation with the antibody. The magnetic particle solution was warmed to 37 °C for 1 min to aggregate, and the aggregated nanoparticles were collected with a magnet. The collected nanoparticles were washed twice with chilled 2% FCS/PBS solution. The premix solution was stored on ice until immediately before use.

**Mice and Neutrophil Separation.** C57BL/6J mice were purchased from Japan Clea, Inc. (Tokyo, Japan) and maintained in the animal facility of the Research Institute, International Medical Center of Japan. All experiments were performed according to the Guidelines for Laboratory Animal Experiments in Research and with the approval of both local ethics committees at the Research Institute, International Medical Center of Japan.

Murine peritoneal neutrophils were prepared as described following ref 21. The peritoneal exudate cells acutely infiltrated in the peritoneal cavity of C57BL/6 mice were induced by intraperitoneal injection with 2 mL of 8% casein in PBS suspension solution. Four hours after injection, cells were collected by washing the peritoneum twice with 5 mL of Hank's balanced salt solution (HBSS). The collected peritoneal fluid

**Scheme 1. Schematic Illustration of Neutrophil Collection**[a]

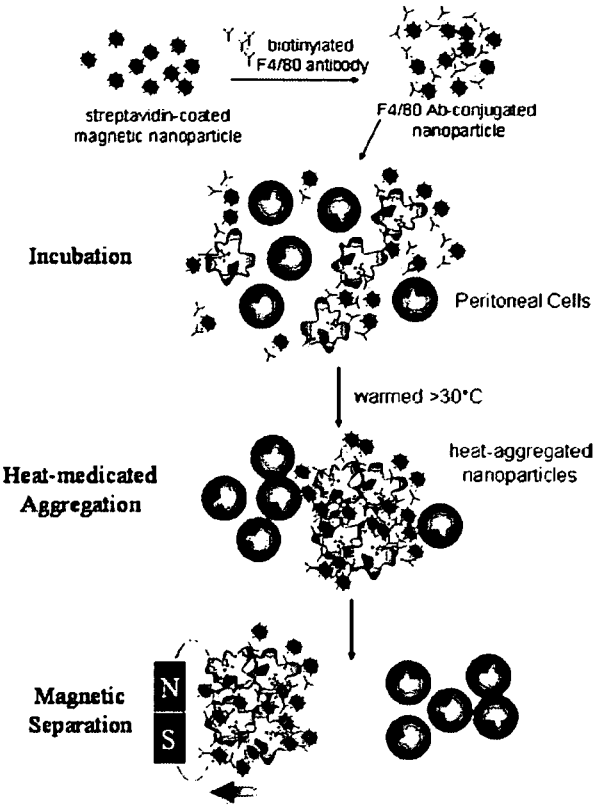


[a] The neutrophils in peritoneal exudate inflammatory cells were collected and the magnetic nanoparticles were prepared before separation as detailed in Materials and Methods.

with HBSS was centrifuged at 800×$g$ for 10 min at room temperature. Then cells were incubated with anti-CD16/32 neutralizing antibody (Pharmingen BD, San Diego, CA) for 20 min on ice to block Fc$\gamma$ receptor-medicated immune responses. The blocked cells were incubated with Therma-Max/anti-F4/80 Ab premix on ice for 20 min and then transferred to a 37 °C water bath and incubated at 37 °C for 1 min to aggregate the magnetic nanoparticles conjugated with cells. The aggregated magnetic nanoparticles with F4/80$^+$ cells were collected under a magnetic field by a magnet (Magna6 stand, Magnabeat Inc.). The purified neutrophils were washed with PBS three times, and the separated neutrophils and macrophage fractions were immediately stained with FITC-conjugated anti-Gr-1 monoclonal Ab (Pharmingen BD), PE-conjugated anti-F4/80 monoclonal Ab (Cedarlane Corp., Ontario, Canada), and PE-conjugated anti-CD11b monoclonal Ab (Pharmingen BD). Then neutrophils were fixed and analyzed by FACS Calibur (BD Biosciences).

## Results and Discussion

**Thermoresponsive Property Magnetic Nanoparticles.** Magnetic beads are one of the most useful tools for cell separation. However, the magnetic-based separation of magnetic particles smaller than 1000 nm is difficult because of the resistance of Brownian movement. Therefore, we coated the magnetic nanoparticles with thermoresponsive polymers that have a lower critical solution temperature (LCST). The polymer-coated magnetic nanoparticles disperse well in an aqueous solution when at a temperature below the LCST and aggregate above the LCST; hence, they easily respond to a magnetic field (*22*,

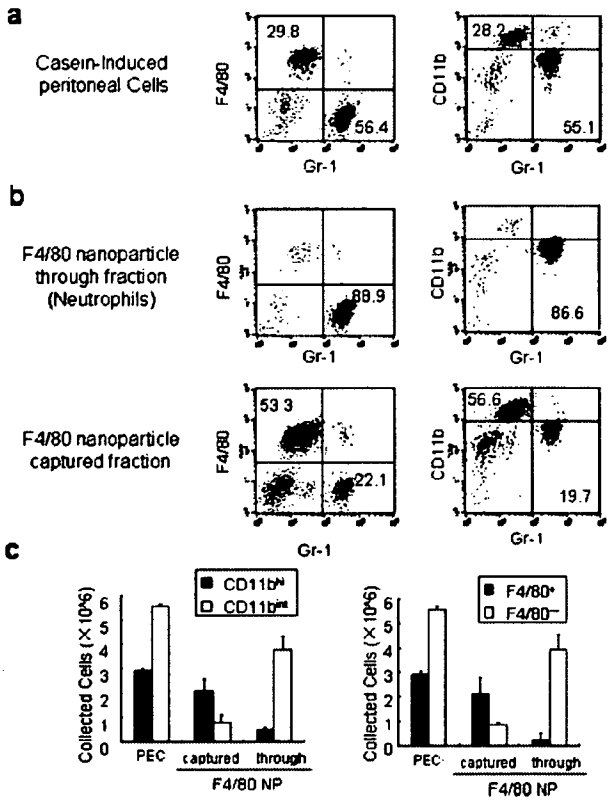


**Figure 2.** Neutrophil separation using magnetic nanoparticles. (a) Peritoneal inflammatory cells stained with FITC-conjugated anti-Gr-1 mAb, PE-conjugated anti-F4/80 mAb, and the PE-conjugated anti-CD11b mAb. The neutrophils were fixed and analyzed by FACS Calibur (BD biosciences). (b) Representative data of magnetic nanoparticle-separated fractions of captured cells and through cells, immediately stained with FITC-conjugated anti-Gr-1 mAb, PE-conjugated anti-F4/80 mAb, and PE-conjugated anti-CD11b mAb, analyzed by FACS Calibur. Gr-1$^{hi}$ CD11b$^{int}$ F4/80$^{-}$ cells are counted as neutrophils, and Gr-1$^{int}$ CD11b$^{hi}$ F4/80$^{+}$ as macrophages. (c) Count of Therma-Max/anti-F4/80-conjugated magnetic nanoparticle-captured and through cell populations. The data are presented as the mean value ± standard deviation of independently performed samples ($n$ = 3).

*23*). The schematic model of the particle's structure is shown in Figure 1a. The particles are expected to be insoluble and responsive to magnetic field when they are heated over 30 °C. As expected, the aggregated nanoparticles show magnetism when warmed in a 37 °C water bath (Figure 1b). To further investigate the thermoresponsive property, the thermal transmittance of the magnetic nanoparticles was measured by a spectrophotometer (Figure 1c). The light transmittance was approximately 100% at low temperature because the nanoparticles were in a dispersed state. The nanoparticles became turbid and lost the transmittance due to floc formation when the temperature increased. The solution dispersed again when they cooled. Thus, the magnetic nanoparticles acquired the property of thermoresponsiveness. To confirm the heat-responsive aggregation, we measured the effective particle size distribution of magnetic nanoparticles in aqueous solution in dispersed and aggregated states, respectively. The dispersed particles show diameters of 167.6 ± 1.5 nm (Figure 1b, blue column). In contrast, the aggregated nanoparticles show 1470.0 ± 85.4 nm diameter distributions at 40 °C (Figure 1d, red column).

**Flow Cytometric Analysis of Target Cells by Magnetic Nanoparticle with Antibody.** The principle of cell separation by Therma-Max LSA Streptavidin (30) magnetic nanoparticles method is to ablate the unwanted cell populations with heat-mediated aggregation of the magnetic nanoparticles. The reaction is schematically shown in Scheme 1. Antibodies against unwanted cell population-specific molecules were first conjugated with thermoresponsive nanoparticles through a biotin−streptavidin complex, which is then bound on the surface of the unwanted cells. The magnetic nanoparticles aggregate and acquire magnetism when the mixture is heated. The unwanted cells are ablated with the aggregated nanoparticles. In this process, only 30 s is enough for aggregation and cell separation.

In order to evaluate the efficiency of the affinity selection of the target cells using Therma-Max LSA Streptavidin (30) magnetic nanoparticles, the separation ability of macrophages and neutrophils from murine peritoneal exudate inflammatory cells was studied. The peritoneal inflammatory cells were induced by intraperitoneal injection of 8% of cow milk casein suspension solution in PBS. The inflammatory cells contain approximately 55% of Gr-1$^{hi}$ CD11b$^{int}$ F4/80$^{-}$ neutrophils and 30% of Gr-1$^{int}$ CD11b$^{hi}$ F4/80$^{+}$ macrophages according to flow cytometric analysis (Figure 2a). To purify the neutrophils in the inflammatory cells, we used magnetic nanoparticles conjugated with anti-F4/80 antibody, because F4/80 antigen is a glycoprotein specifically expressed on the cell surface of macrophages and monocytes. After reaction, the cells captured on F4/80-magnetic nanoparticles were drawn and accumulated under the magnetic field. After the separation procedure, the target neutrophils were collected and concentrated; the noncaptured fraction included more than 85% Gr-1$^{hi}$ CD11b$^{int}$ F4/80$^{-}$ neutrophils (Figure 2b). This result suggests that ablation of macrophages by magnetic nanoparticles is more suitable for neutrophil collection. Surprisingly, the macrophage-rich fraction could also be collected from the captured fraction; the captured cell fraction contained approximately 20% Gr-1$^{hi}$ CD11b$^{int}$ F4/80$^{-}$ neutrophils and 55% Gr-1$^{int}$ CD11b$^{hi}$ F4/80$^{+}$ macrophages after one cycle of separation (Figure 2b). Therefore, Therma-Max LSA Streptavidin (30) magnetic nanoparticles would be useful to separate a specific cell population. The nanoparticles are retained on the cell surface, while unlabeled cells pass through. The retained particles are dropped off from the surface after 1 h of culture at 37 °C (data not shown). These cells can be also used for both flow cytometric and microscopic analysis.

In conclusion, the present study demonstrates the high potential of a new technique to collect and purify both labeled (positive selection) and unlabeled (depletion) cells with thermoresponsive magnetic nanoparticles.

## Acknowledgment

We thank Mr. Yu Muraoka (Faculty of Engineering, Kobe University) for his technical assistance. This work was supported partly by a domestic research fellow grant from the Japan Society for the Promotion of Science (A.H.) and partly by a grant "Research on Nanotechnical Medical" (H19-nano-012) from Ministry of Health, Labor and Welfare (K.Y.).

## References and Notes

(1) Valiev, R. Materials science: Nanomaterial advantage. *Nature* **2002**, *419*, 887−889.

(2) Hsieh, J. M.; Ho, M. L.; Wu, P. W.; Chou, P. T.; Tsai, T. T.; Chi, Y. Iridium-complex modified CdSe/ZnS quantum dots; a conceptual design for bi-functionality toward imaging and photosensitization. *Chem. Commun. (Cambridge)* **2006**, (*6*), 615−617.

(3) Voura, E. B.; Jaiswal, J. K.; Mattoussi, H.; Simon, S. M. Tracking metastatic tumor cell extravasation with quantum dot nanocrystals and fluorescence emission-scanning microscopy. *Nat. Med.* **2004**, *10* (9), 993−998.
(4) Dubertret, B.; Skourides, P.; Norris, D. J.; Noireaux, V.; Brivanlou, A. H.; Libchaber, A. In vivo imaging of quantum dots encapsulated in phospholipid micelles. *Science* **2002**, *298* (5599), 1759−1762.
(5) Akerman, M. E.; Chan, W. C.; Laakkonen, P.; Bhatia, S. N.; Ruoslahti, E. Nanocrystal targeting in vivo. *Proc. Natl. Acad. Sci. U.S.A.* **2002**, *99* (20), 12617−12621.
(6) Ebbesen, M.; Jensen, T. G. Nanomedicine: techniques, potentials, and ethical implications. *J. Biomed. Biotechnol.* **2006**, *2006* (5), 51516.
(7) Freitas, R. A., Jr. Nanotechnology, nanomedicine and nanosurgery. *Int. J. Surg.* **2005**, *3* (4), 243−246.
(8) Caruthers, S. D.; Wickline, S. A.; Lanza, G. M. Nanotechnological applications in medicine. *Curr. Opin. Biotechnol.* **2007**, *18* (1), 26−30.
(9) Kim, K. Y. Research training and academic disciplines at the convergence of nanotechnology and biomedicine in the United States. *Nat. Biotechnol.* **2007**, *25* (3), 359−361.
(10) Eaton, M., Nanomedicine: industry-wise research. *Nat. Mater.* **2007**, *6* (4), 251−253.
(11) Navalakhe, R. M.; Nandedkar, T. D. Application of nanotechnology in biomedicine. *Indian J. Exp. Biol.* **2007**, *45* (2), 160−165.
(12) Arayne, M. S.; Sultana, N. Review: nanoparticles in drug delivery for the treatment of cancer. *Pak. J. Pharm. Sci.* **2006**, *19* (3), 258−268.
(13) Lin, H.; Datar, R. H. Medical applications of nanotechnology. *Natl. Med. J. India* **2006**, *19* (1), 27−32.
(14) Furukawa, H.; Shimojyo, R.; Ohnishi, N.; Fukuda, H.; Kondo, A. Affinity selection of target cells from cell surface displayed libraries: a novel procedure using thermo-responsive magnetic nanoparticles. *Appl. Microbiol. Biotechnol.* **2003**, *62*, 478−483.
(15) Janeway, C., *Immunobiology*, 5th ed.; Garland Sciences: London, 2001.
(16) Pham, C. T. Neutrophil serine proteases: specific regulators of inflammation. *Nat. Rev. Immunol.* **2006**, *6* (7), 541−550.
(17) Aratani, Y.; Kura, F.; Watanabe, H.; Akagawa, H.; Takano, Y.; Suzuki, K.; Dinauer, M. C.; Maeda, N.; Koyama, H. Critical role of myeloperoxidase and nicotinamide adenine dinucleotide phosphate-oxidase in high-burden systemic infection of mice with *Candida albicans*. *J. Infect. Dis.* **2002**, *185* (12), 1833−1837.
(18) El Messaoudi, K.; Verheyden, A. M.; Thiry, L.; Fourez, S.; Tasiaux, N.; Bollen, A.; Moguilevsky, N. Human recombinant myeloperoxidase antiviral activity on cytomegalovirus. *J. Med. Virol.* **2002**, *66* (2), 218−223.
(19) Klebanoff, S. J.; Coombs, R. W.; Viricidal effect of polymorphonuclear leukocytes on human immunodeficiency virus-1. Role of the myeloperoxidase system. *J. Clin. Invest.* **1992**, *89* (6), 2014−2017.
(20) Moguilevsky, N.; Steens, M.; Thiriart, C.; Prieels, J. P.; Thiry, L.; Bollen, A. Lethal oxidative damage to human immunodeficiency virus by human recombinant myeloperoxidase. *FEBS Lett.* **1992**, *302* (3), 209−212.
(21) Hoshino, A.; Nagao, T.; Ito-Ihara, T.; Ishida-Okawara, A.; Uno, K.; Muso, E.; Nagi-Miura, N.; Ohno, N.; Tokunaka, K.; Naoe, S.; Hashimoto, H.; Yasuhara, M.; Yamamoto, K.; Suzuki, K. Trafficking of QD-conjugated MPO-ANCA in Murine Systemic Vasculitis and Glomerulonephritis model mice. *Microbiol. Immunol.* **2007**, *51* (5), 551−566.
(22) Kondo, A.; Kanuma, H.; Higashitani, K. Development and application of thermo-sensitive magnetic immunomicrospheres for antibody purification. *Appl. Microbiol. Biotechnol.* **1994**, *41*, 99−105.
(23) Kondo, A.; Fukuda, H. Preparation of thermo-sensitive magnetic hydrogel microsperes and application to enzyme immobilization. *J. Ferment. Bioeng.* **1997**, *84*, 337−341.

Received June 12, 2007. Accepted August 30, 2007.

BP070185E

Journal of Nanophotonics, Vol. 1, 013516 (10 July 2007)

# Fluorescence millisecond oscillation in polar solvents regulates fluorescence intensity of colloidal quantum dots' solution

**Akiyoshi Hoshino[a,b], Kazumi Omata[c], Seiichi Takami[d], Tadafumi Adschiri[d], Naofumi Terada[e], Takashi Funatsu[e], Masato Yasuhara[b] and Kenji Yamamoto[a,b]***

[a] International Clinical Research Center, Research Institute, International Medical Center of Japan, Toyama 1-21-1, Shinjuku-*ku*, Tokyo 162-8655, Japan

[b] Department of Pharmacokinetics, Pharmacodynamics and Hospital Pharmacy, Tokyo Medical and Dental University Graduate School of Medicine, Tokyo 113-8510, Japan

[c] Department of Clinical Research and informatics, Research Institute, International Medical Center of Japan, Tokyo 162-8655, Japan

[d] Research Center of Sustainable Materials Engineering, Institute of Multidisciplinary Research for Advanced Materials, Tohoku University Graduate School of Engineering, Sendai 980-8577, Japan

[e] Laboratory of Bioanalytical Chemistry, Graduate School of Pharmaceutical Sciences, The University of Tokyo, Tokyo 113-0033, Japan

* Corresponding author: backen@ri.imcj.go.jp

**Abstract.** Quantum Dots (QDs) have been used in life science study because of their higher emission and photostability. Although physicochemical and biological properties of QDs were varied dramatically by the surface modification of QDs, little is known about the reason why the photoluminescence intensity (PLI) of QDs was changed by surface modification. We report on the millisecond-span change of PLI of QD's collective fluorescence oscillation. QDs covered with carboxylic acid and hydroxyl groups show enhanced PLI by adding $NaN_3$, whereas QDs with amine showed less. Removal of $NaN_3$ from QD solution abrogated the enhanced PLI. In addition, observation on evanescent field revealed that addition of antioxidants induced enhanced oscillation of QDs. Furthermore, the blinking count at one millisecond was also increased by addition of antioxidants. However the oscillation enhancement is observed in both aqueous solution and polar organic solvents but not in nonpolar organic solvents, indicating that PLI of QD was varied by the interaction between QDs and their environmental solvents. These millisecond oscillation mechanism was independent of "on" and "off" events which were conventionally known as "blinking". Taken together, the fluorescent emission of colloidal QDs is affected by both surface-covered colloidal molecules and external solvents around at millisecond span interaction.

**Keywords:** quantum dots, blinking, single molecular imaging, polar organic solvents, millisecond oscillation.

## 1 INTRODUCTION

Nowadays, colloidal nanocrystal quantum dots (QDs) are widely used in biological study because QDs are attractive fluorophores for multicolor imaging due to broad absorption and narrow emission spectra and brighter and far more photostable than organic dyes. Many advanced improvements on surface modification of QDs enable to promote a lot of biological experiments. Although physicochemical and biological properties of QDs were varied dramatically by the surface modification of QDs [1-3], little is known about the reason why the photoluminescence intensity (PLI) of QDs was also changed by surface modification. We

 [DOI: 10.1117/1.2767608]
Received 18 Apr 2007; accepted 4 Jul 2007; published 10 Jul 2007 [CCC: 19342608/2007/$25.00]

previously reported that QDs were applied for some biological experiments; long-term multicolor cell imaging [4,5], single cell tracking in live cells [6,7], microorganism observation in living cells [8,9], single bacterial antigen detection under evanescent emission field [10], and even in cancer immunotherapy with QDs [11,12]. When QDs are observed under the steady laser illumination such as evanescent fields, the photoluminescence of single QDs shows fluctuations, called blinking [11,12]. Blinking is one of the specific characters of single fluorescent nanomaterials, and many researchers previous focused on bright fraction and on dark fraction events in the span of several minutes [13-16].

We found that the preservative chemical, sodium azide ($NaN_3$), in storage buffer have an ability to change fluorescent intensity of QDs. We assumed it could be explained by the change of blinking, but in failed. Therefore in this paper, we focused on the short time phenomenon within a millisecond span; both surface-covered colloidal molecules and environmental solvents around QDs interact and affect the fluorescent emission at a span of milliseconds.

## 2 EXPERIMENTAL DETAILS

### 2.1 Preparation of surface-modified nanocrystal QDs

ZnS-coated CdSe nanocrystal QDs enfolded into the micelle of n-trioctylphosphine oxide (TOPO) (fluorescence wavelength: approximately 522 nm, emitted green) were synthesized by a known inversed-micelle method [17]. In brief, QDs were dissolved into chloroform in 4ml-volume flask and dihydrolipoic acid (DHLA), 2-aminoethanethiol (cysteamine hydrochloride), or 3-mercapto 1,2-propanediol (thioglycerol) were added in order to replace surface TOPO in these molecules [18]. After moderately heating for 24 hours under reflux conditions with an oil bath whose temperature was set at 90 °C, methanol was dropped to the flask and mixed until the QDs were deposited. The turbid solution was centrifuged and washed with acetone twice. Next, distilled water was added to the QD precipitated residue. QD solution was applied to a Sephadex G-25 column (PD-10, Amersham Biosciences, Piscataway, NJ) to remove impurities, and then flow-through was purified using an ultra-filtration membrane (Amicon ultra; NMWL =5 kDa, Millipore, Concord Road Billerica, MA) to remove detached low molecular ingredients such as DHLA, cysteamine and thioglycerol. Finally, purified QD solution was powderized by vacuum distillation. QDs were reconstituted in distilled water and filtrated with a 0.1-μm filter (Millipore) immediately before use.

### 2.2 Evanescent field assay

QD-COOH, QD-OH, and QD-$NH_2$ were dissolved in purified water. Then QD solution was warmed to 50 °C and mixed with one-fifth volume of 5 % agarose solution. The mixture was dropped on the APS-coated slide glass (Matsunami glass Indusrtiy, Osaka, Japan) and immediately embedded with 0.12 mm-thickness coverslips (Matsunami Glass Industries). The packaged samples were then chilled to with or without 1 μM $NaN_3$ solution. Millisecond oscillation of QD was observed on the evanescent field of total-reflective fluorescent microscopy. The samples were excited with an argon laser (488 nm) on the evanescent field, and observed through dichroic mirrors (DM505) and emission filters on an Olympus IX-70 equipped with total-interanal reflective fluorescent microscopy. The laser beam was injected on the coverslip at 58.4 ~ 64.2 degree to the optical axis giving a decay constant of the evanescent field of 48-62 nm. The beam was focused on the periphery of the back focal plane of a 100x objective lens with NA of 1.65 with high refractive index immersion oil (Olympus Corporation). The filter cube contained a 488/10 laser clean-up filter in the excitation position, and emission signals were separated using two kinds of optical splitters; Ch1was

with 510-550 band-pass, and Ch2 was with > 610 long-pass emission filters; the red (Ch2) and green (Ch1) images were simultaneously imaged side by side on observed with a fiber-coupled CCD camera (FASTCAM® MAXI-$I^2$, Photoron corp., Tokyo, Japan). Millisecond oscillation was by captured every one millisecond Span by using MetaMorph® software (Universal Imaging Corporation, Marlow, Buckinghamshire, UK), and numeric conversion was performed with NIH-Image software. The oscillation frequency was analyzed and calculated by Fourier transform.

## 3 RESULTS

### 3.1 External condition of nanocrystal QD solution affect the photoluminescence

We assumed that the surrounding environmental molecules could affect the emission properties of QDs, the same as shown in the change of physicochemical properties and cytotoxicity [19]. We have changed the surface-covered organic molecules of QD to bind biological molecules functionally and stably. These data suggested that the electric charge of QD was significantly concerned with their augmentation/diminishment of fluorescent intensity by $NaN_3$. Next, we examined whether other preservative molecules have an ability to enhance the fluorescent intensity of QD (Fig.1b). Fluorescence intensity of nanocrystal QDs was also enhanced by some kinds of antioxidant agents such as 2-mercaptoethanol and dithiothreitol. In contrast, an oxidant chemical 1H-pyrrole diminished the fluorescent intensity. However, ascorbic acid and D-sorbitol, which are frequently used as food antioxidant, diminished the fluorescence, suggesting that electron leakage of QDs via the ionization of surface-covered molecules regulate the fluorescent enhancement. To investigate the possibility that $NaN_3$ directly binds the surface of QDs, we compared the fluorescence before and after removal of $NaN_3$. QD solution with $NaN_3$ was purified by dialysis with ulteracentrifuge filter to remove uncomplexed $NaN_3$ in QD solution. Removal of $NaN_3$ by dialysis from the solution recovered the QDs' augmented/diminished fluorescence (Fig.1c), implying that no direct chemical interaction of $NaN_3$ (e.g, covalent bond and ionic complex) was formed on the surface of QDs. Thus, the solutes around QD-solution influenced the fluorescence intensity of QDs. These results suggest that not only the surface covered molecules but also surrounding external environmental solutes around QD solution regulate the fluorescence intensity.

### 3.2 On- and Off-phases of nanocrystal QD oscillation

These results prompted us to investigate whether blinking frequency of QDs was also enhanced by the addition of $NaN_3$ into the QD-COOH solution, because the intermittence in fluorescent emission is known as blinking [20-22]. We compared the blinking on each QD under a fluorospectrometry (Fig. 2a) with an evanescent fluorescent field (Fig. 2b) by ultra sensitive high-speed camera. We observed sudden hopping enhancement of photoluminescence intensity in a span of millisecond. Notably, the millisecond oscillation we observed is still continued after transition from "on-phase" to "off-phase" of QD (Fig 2b). We defined this phenomenon as millisecond oscillation. Millisecond oscillation is different phenomenon to conventional photo-intermittence called blinking.

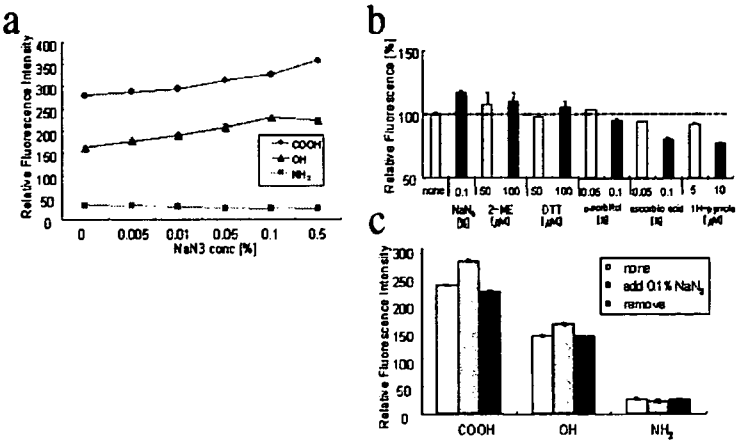


Fig. 1. External environmental condition on QDs varies fluorescence intensity. (a), $NaN_3$ in aqueous solution augment/diminish the fluorescence intensity of QD. The fluorescence intensity of 100 μM of QD-COOH (red circle), QD-OH (blue triangle), and QD-$NH_2$ (green square) were measured in the presence of $NaN_3$ at the range of 0- 0.5 % concentrations. (b), Fluorescence intensity of QD-COOH was changed by the antioxidants in aqueous solution. (c), $NaN_3$ Removal by dialysis recovered the augmented/diminished fluorescence intensity by the effect of $NaN_3$. QD solutions with 0.1 % $NaN_3$ were dialyzed by ultrafiltration membrane. The concentration of collected solution was adjusted with adequate volume of distilled water. Data are the mean aggregation area ± one SD of triplicate experiments.

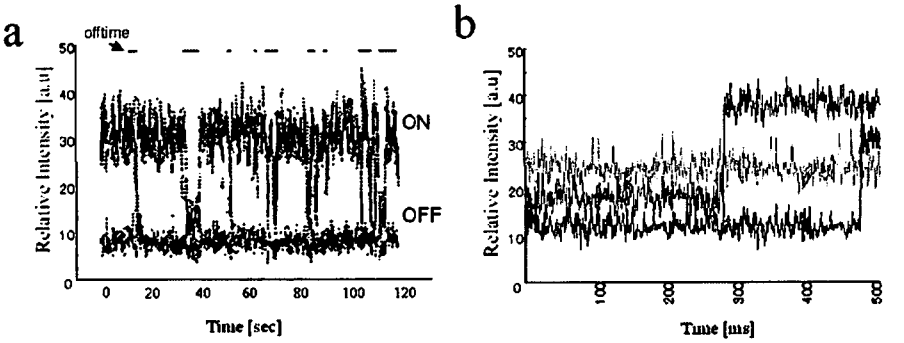


Fig. 2. The mechanism of the millisecond oscillation is different from that of blinking. (a), A blinking change of QD-COOH fluorescence intensity in aqueous solution. Fluorescence intensity was continuously measured for 120 sec with a fluorospectrometer. The red line upper graph indicates" off" phase of blinking. (b), The millisecond oscillation of QD-COOH in aqueous solution was observed on the evanescent field with ultra sensitive high-speed fiber-coupled CCD camera (FASTCAM® MAXI-$I^2$, Photoron corp., Tokyo, Japan). *x*-axis indicates the time and *y*-axis indicates the relative fluorescence intensity. Red, blue, and yellow lines that indicate the emission from individual QD during the on-off switching phase (n=3) were overlaid. Green line indicates the photoemission of "on-phase".

### 3.3 $NaN_3$ in aqueous solution change the QD-oscillation

Next we investigated the relationship between $NaN_3$-dependent fluorescence enhancement and the millisecond oscillation. We observed whether the millisecond oscillation was also

enhanced by the addition of $NaN_3$ into the QD-COOH solution. The millisecond oscillation was also enhanced by the addition of $NaN_3$. The photoluminescence frequency of fluorescence millisecond oscillation that was observed on the evanescent field of total-reflective fluorescent microscopy with a fiber-coupled CCD camera (Movie 1) was enhanced by the addition of $NaN_3$ in QD-solution (Movie 2).

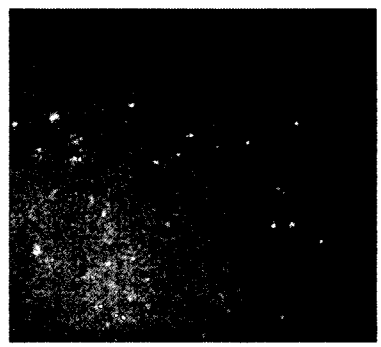

Video 1. QD-COOH solution was embedded into the 1% agarose gel without $NaN_3$. Millisecond oscillation of QD was observed on the evanescent field of total-reflective fluorescent microscopy with a fiber-coupled CCD camera (FASTCAM® MAXI $I^2$, Photoron Corp., Tokyo, Japan) by capturing at a span of every one mllisecond (QuickTime, 1.52 MB).

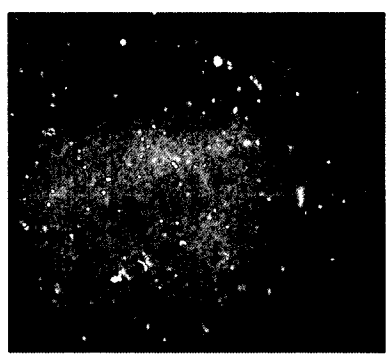

Video 2. QD-COOH solution was embedded into the 1% agarose gel containing 1 μM $NaN_3$. Millisecond oscillation of QD was observed on the evanescent field of total-reflective fluorescent microscopy with a fiber-coupled CCD camera (FASTCAM® MAXI $I^2$, Photoron Corp., Tokyo, Japan) by capturing at a span of every one mllisecond (QuickTime, 883 KB).

To support this, the analyzed power spectrum of QD-COOH before and after $NaN_3$ indicated that the photoluminescence frequency of fluorescence millisecond oscillation was also increased (Fig.3). This result suggests that $NaN_3$ in QD-solution has an ability to increase the photon emission from QDs. The same results were observed in QD-OH solution, but not QD-$NH_2$ solution (data not shown). This is consistent with the results that QD-$NH_2$ has no activity to enhance the fluorescent intensity.

### 3.4 Solvent-Surface interaction regulates the oscillation of nanocrystal QDs

Next we determine the effect of solvents on millisecond oscillation. To investigate the possibility that aqueous solvents were implicated to the millisecond oscillation, QD-COOH was dispersed and fixed on the surface of cover slip and filled with some organic solvents. We assumed that the oscillation of QD was not observed in chloroform. Contrary to our expectation, the QD-oscillation was also observed even in chloroform (Fig. 4a). Then we hypothesized that polarity of the organic solvents was also operated as the electron donor in the solution. In the non-polar organic solution such as toluene, each QD displays no detectable fluorescent oscillation (Fig. 4b). The results suggest that both solutes and solvents that surrounded by QDs may function as the donor/interceptor of excited electron on nanocrystal QDs.

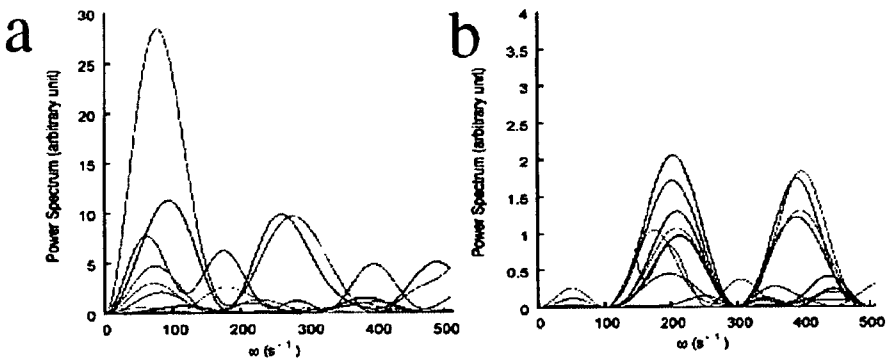


Fig. 3. Exposure to $NaN_3$ changes the frequency of millisecond oscillation. QD-COOH was embedded into the 1 % agarose gel (a) with or (b) without 1 μM $NaN_3$. Millisecond oscillation of QD was observed on the evanescent field of total-reflective fluorescent microscopy. Millisecond oscillation was observed with a CCD camera unit FASTCAM® by captured at the span of every one millisecond. The oscillation frequency of each monodispersed QD is analyzed by Fourier Transform. *x*-axis indicates oscillation frequency [s-1] of QD. Each line indicates individual QD (n=20). One of three independent experiments is presented.

### 3.5 Discussion

The theory that electron transfer processes regulates the power-law distribution for the lifetime of a blinking of QDs has already proposed [23]. We first demonstrated that the electron condition on the core of QD, beside the QD covered molecules, and even around QD external environments by observation of millisecond oscillation, implying that emission of QD depends on at least these factors; surface-covered substance, the solvent and solutes in solution, specified the fluorescence activity of QD particle. The studies demonstrated here suggest that QD property depends on multiple factors derived from both the inherent physicochemical properties of QDs and environmental conditions. For example, we found that QD properties like QD size, charge, concentration, outer coating bioactivity (capping material and functional groups), and oxidative, photolytic, and mechanical stability are each factors that, collectively and individually, can determine the toxicity of QD [20, 24]. We can overcome the reduction of cytotoxicity by changing the physicochemical characteristics, functional coating and core stability of QDs. It has no doubt that the photoluminescence property of QDs also depend on the environmental conditions around QDs [25]. In addition, our result supports the possibility that the brightness of whole QD particle can be also